



ELSEVIER

Available online at www.sciencedirect.com

SciVerse ScienceDirect

Proceedings of the Combustion Institute 34 (2013) 1143–1149

Proceedings
of the
Combustion
Institutewww.elsevier.com/locate/proci

Combustion chemistry of $\text{Ti}(\text{OC}_3\text{H}_7)_4$ in premixed flat burner-stabilized $\text{H}_2/\text{O}_2/\text{Ar}$ flame at 1 atm

A.G. Shmakov^a, O.P. Korobeinichev^{a,*}, D.A. Knyazkov^a,
A.A. Paletsky^a, R.A. Maksutov^{a,b}, I.E. Gerasimov^a, T.A. Bolshova^a,
V.G. Kiselev^{a,b}, N.P. Gritsan^{a,b}

^a Institute of Chemical Kinetics and Combustion SB RAS, Novosibirsk, Russia

^b Novosibirsk State University, Novosibirsk, Russia

Available online 19 June 2012

Abstract

The flame structure of the premixed $\text{H}_2/\text{O}_2/\text{Ar}$ mixture (13%/14.5%/72.5% vol.) with and without 0.12 vol.% of titanium tetraisopropoxide ($\text{Ti}(\text{OC}_3\text{H}_7)_4$) has been studied experimentally using the flame-sampling molecular beam mass-spectrometry and the microthermocouple techniques. The flame was stabilized on a flat burner at 1 atm. The temperature and concentration profiles for H_2 , O_2 , H_2O , and $\text{Ti}(\text{OC}_3\text{H}_7)_4$ have been measured. The mass peak intensity profiles of the titanium-containing species TiO_2 , HTiO_2 , TiO , HTiO , Ti , TiH , Ti_2O_3 , TiO_3 have been measured as well. The experimental results were analyzed using kinetic modeling and quantum chemical calculations. It was established that hydrolysis of $\text{Ti}(\text{OC}_3\text{H}_7)_4$ is the dominating primary reaction of its decomposition in the flame. The rate constant of hydrolysis was estimated to be $k = 2 \times 10^{12} \exp(-6160/T) \text{ mol}^{-1} \text{ cm}^3 \text{ s}^{-1}$. The results of quantum chemical computations support this conclusion. On the basis of concentration profiles of the Ti-containing intermediates, the schematic mechanism of the $\text{Ti}(\text{OC}_3\text{H}_7)_4$ conversion in the flame has been proposed.

© 2012 The Combustion Institute. Published by Elsevier Inc. All rights reserved.

Keywords: Flame structure; Titanium dioxide; Titanium tetraisopropoxide; Probing molecular beam mass spectrometry; Reaction mechanism

1. Introduction

Titanium dioxide (TiO_2) is widely used as a photocatalyst, semiconductor, a special coating material for glass and ceramic materials, as well as a white pigment. Moreover, TiO_2 is a promising compound for application in the dye-

sensitized solar cells (DSSC) [1,2] and gas sensors [3,4]. One of the challenges in application of TiO_2 is development of the procedures to produce nanocrystalline materials with required properties. A variety of procedures for manufacturing nanoparticles of TiO_2 have been developed, including the sol-gel process [5,6], electrochemical methods [7], chemical deposition from the gas phase [8]. However, these methods have some disadvantages. For instance, most of procedures are multi-stage, and the produced nanoparticles have amorphous structure. In addition, nanoparticles produced by these methods contain impurities.

* Corresponding author. Address: Institute of Chemical Kinetics and Combustion, 3 Institutskaya street, Novosibirsk 630090, Russia. Fax: +7 383 3307350.

E-mail address: korobein@kinetics.nsc.ru (O.P. Korobeinichev).

This deteriorates the material quality and/or raises production costs.

The TiO₂ can be also synthesized in the flame. This method allows one-step production of mesoporous film of TiO₂ nanocrystals on a substrate [9]. By varying the composition of the reagents, it is possible to produce nanoparticles of high purity in the required crystalline phase with a desired size and narrow size distribution. Analysis of the literature demonstrates that properties of the TiO₂ films strongly depend on the flame configuration (e.g., diffusion [10] or premixed flame [11–14]), flame stabilization technique (on a porous burner, a cooled substrate, etc.), and on the experimental conditions (pressure, stoichiometry of the mixture, and concentration of precursor) [15–24].

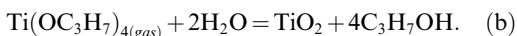
TiCl₄ and different titanium alkoxides, mainly titanium tetraisopropoxide (TTIP, Ti(OC₃H₇)₄), are generally used as precursors for production of TiO₂ in flames. The detailed chemical mechanism and rate constants of the elementary reactions are crucial for deep understanding and modeling of processes leading to formation of TiO₂ nanoparticles in the flame. Unfortunately, these data are rather scarce. In the case of titanium tetrachloride, the kinetic mechanism of TiCl₄ oxidation in the flame has been studied both theoretically [25–29] and experimentally [30,31].

TTIP is a more convenient precursor than TiCl₄ as it does not contain chlorine atoms. However, the mechanism and kinetics of the TTIP thermal decomposition are almost unexplored. First experimental results on the kinetics of TTIP thermal decomposition have been reported by Okuyama et al. [32], who studied the thermolysis of TTIP vapor in a flow reactor in the temperature range 500–660 K. The authors have proposed the overall process of TTIP consumption [32].



By measuring the kinetics of propylene formation, they estimated the effective first-order rate constant of TTIP thermal decomposition and its temperature dependence: $k = 3.96 \times 10^5 \exp(-8479.7/T) \text{ s}^{-1}$.

Later, Seto et al. [33] studied the hydrolysis of TTIP leading to formation of TiO₂ and isopropyl alcohol according to the scheme



However, this paper is written very unclear, and we were not even able to extract the value of the rate constant corresponding to this formal trimolecular reaction (b).

Thus, the existing experimental data on the primary reactions of the TTIP thermal decomposition are indeed incomplete. The estimated pre-exponential factor of the TTIP consumption rate constant (a) is unreasonably low. This is the indication of the complex mechanism of the

process. Moreover, the kinetics of the TTIP conversion in the flame has never been studied.

Our paper is devoted to the study of the TTIP combustion in the hydrogen flame. The main goal is to determine the kinetics of the initial stage of the TTIP decomposition and to identify the Ti-containing final products of the TTIP combustion. For this purpose, we studied the flame structure experimentally and by means of numerical modeling. In addition, the quantum chemical calculations at the DFT level were employed to support our findings.

2. Experimental and computational details

2.1. Experimental setup

The flame of H₂/O₂/Ar (0.13/0.145/0.725) with the equivalence ratio $\phi = 0.45$ was stabilized on a flat burner. The burner was a perforated copper disk with the diameter 16 mm (the disk thickness being 3 mm, the hole diameter 0.5 mm, and a hole spacing 0.7 mm), mounted in a brass case with a water jacket. The temperature of the burner case was maintained at 128° C by a thermostat connected with the water jacket. The combustible mixture was prepared by mixing gas flows immediately in the gas pipeline connected with the burner. The composition of the combustible mixture was monitored using mass flow controllers (MKS Instruments, Inc.). The gas purity (O₂, Ar, H₂) was not less than 99.99%. The flow volume of the combustible mixture was 200 cm³/s (at the temperature 20° C). Titanium tetraisopropoxide (Ti(OC₃H₇)₄, Sigma–Aldrich, purity >98%) was added to the flow of the combustible mixture by a passing part of the argon flow through a bubble flask with liquid Ti(OC₃H₇)₄. The bubble flask was immersed into the thermostat at the temperature 90° C. The concentration of TTIP in the combustible mixture was calculated using the mass loss kinetics of the bubble flask weight over a set period of time with the set flow volume. The concentration of the Ti(OC₃H₇)₄ in the gas phase at the output of the burner was $0.12 \pm 0.01\%$ of the volume.

A flame-sampling molecular beam mass spectrometric setup [34] was used to measure the intensities of mass peaks corresponding to various species in the flame as a function of the height above the burner (HAB). The precision of burner positioning against the probe was 0.01 mm and was controlled by a cathetometer.

A ceramic (Al₂O₃) conic probe with the orifice diameter 0.14 mm and the wall thickness near the orifice 0.14 mm was used; the interior angle of the conic part was 40°. A probe was vertically inserted into the flame. Note that ceramic probe of this type has been used for the first time to measure the flame structure. To substantiate applicability

of this probe to the study of the flame structure, we measured the concentration profiles of different species, including H and OH radicals in H₂/O₂/Ar flame ($\phi = 1.1$) and compared results with those measured by a typical quartz probe (Fig. S1, Supplemental data) and those obtained by a numerical modeling. A good agreement of all those data indicates that an Al₂O₃ probe can be successfully applied for measuring the flame structure.

In the flame with Ti(OC₃H₇)₄ additive, the probe orifice got stuck with TiO₂ particles. Therefore, it was necessary to clean it regularly with abrasive paper. A ceramic probe survived a much greater number of cleaning cycles than a quartz probe used previously for similar measurements.

The accuracy of the species concentration measurements in the flame is determined by a number of factors. The most important one is the accuracy of measuring the mass peak intensities. The latter depends on the concentration of the corresponding component in the flame and on the intensity of the background mass spectrum.

Calibration of the concentrations for the major species measured in the flame was carried out directly in the original combustible mixture (the composition of the mixture was determined with a relative accuracy $\pm 1\%$) and in the combustion products (in the post flame zone). In the latter case, concentrations were calculated under the assumption of complete hydrogen burning. The experimental relative accuracy of the mass spectrometric concentration measurements during probe sampling was $\sim 5\%$ for H₂ and O₂, and $\sim 20\%$ for Ti(OC₃H₇)₄. Note that in the case of TTIP, the accuracy is poor; therefore, the concentration profiles were obtained by averaging the results of several (at least 3) experiments.

Calibration of the concentrations of TiO₂, HTiO₂, TiO, HTiO, Ti, TiH, Ti₂O₃, and TiO₃ was not performed, since these species are labile and the thermochemical parameters are not available for most of them. The results are presented as intensity profiles of the corresponding mass peaks, normalized for the intensity of the reference gas (argon) peak.

The temperature profile across the flame zone was measured by a platinum–platinum–rhodium (Pt–Pt10%Rh) Π -shaped thermocouple with a wire diameter of 0.02 mm. The shoulder of the thermocouple was 12 mm. The thermocouple surface was coated with SiO₂ to prevent catalytic processes. The total diameter of the thermocouple with the coating was 0.03 mm. Springs were used to prevent possible deflection of the wires due to thermal expansion of the metal. The heat losses from the thermocouple due to radiation were estimated by the method proposed by Kaskan [35]. The total uncertainty in the flame temperature measurements did not exceed 30 K.

Due to experimental difficulties (deposition of TiO₂ particles on the thermocouple), the thermocouple measurements were made only in the flame without TTIP. In that case, a good agreement was found between experimental and simulated temperature profiles. Apart from this, we measured the concentrations of H₂, O₂, H₂O in the flame reaction zone with and without TTIP additive and found virtually no significant difference. Therefore, we applied the calculated temperature profile (for flame doped with TTIP additive) to the rate constant calculations. The temperature profile was calculated using the CHEMKIN code and the detailed reaction mechanism, as well as the thermochemistry and transport data. The initial conditions, including the composition of the fresh combustible mixture, the mass flow rate and the temperature, were used for simulation.

2.2. Theoretical modeling

The flame structure was simulated using CHEMKIN suite of programs (Sandia National Laboratory, USA) [36,37] and Konnov's detailed reaction mechanism of hydrogen combustion [38].

The reaction of thermal decomposition of the TTIP was added to the mechanism of [38]; the standard enthalpies of formation of TTIP and TiO₂ were taken from the NIST database [39].

The primary decomposition reactions of TTIP were studied at the B3LYP/6–311++G(2df,p) level of theory [40,41]. All calculations were performed using Gaussian 03 suite of programs [42].

3. Results and discussion

The intensities of the mass peaks with $m/z = 2$, 18, and 32 (H₂, H₂O, and O₂, respectively) were measured at the ionizing electron energy of 16.5 eV. The corresponding concentration profiles are shown in Fig. 1. It was found that the addition of 0.12% TTIP to the combustible mixture did not affect essentially on the width of the consumption zone of the reagents (H₂ and O₂). The concentration profile of TTIP (Fig. 2) was measured using the characteristic peak $m/z = 269$ with the ionizing electron energy of 21.0 eV. Figure 2 (dots) demonstrates that the Ti(OC₃H₇)₄ transformation zone is of about 1 mm width and is comparable with the consumption zone of the main reactants–H₂ and O₂.

As already mentioned in the Introduction, two reactions were proposed to describe the thermolysis and hydrolysis of Ti(OC₃H₇)₄ (pathways (a) and (b), correspondingly) [32,33]. We tried to model the kinetics of Ti(OC₃H₇)₄ transformation in the flame using the effective rate constant of pathway (a). Figure 2 (curve 1) shows that the experimental results cannot be described using only reaction (a) with the rate constant proposed

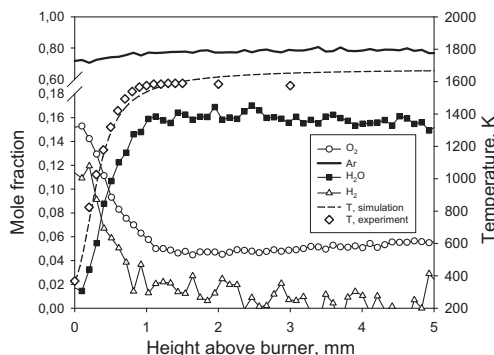


Fig. 1. Species concentration and temperature profiles in $\text{H}_2/\text{O}_2/\text{Ar}$ flame with $\text{Ti}(\text{OC}_3\text{H}_7)_4$ additive.

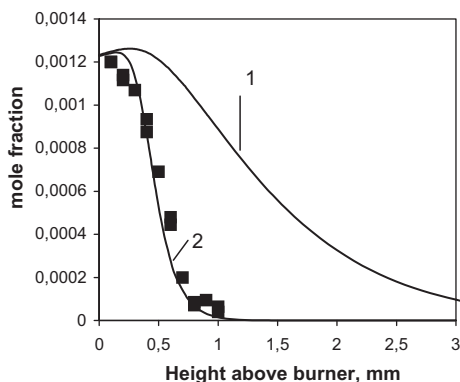


Fig. 2. Concentration profile of $\text{Ti}(\text{OC}_3\text{H}_7)_4$ in $\text{H}_2/\text{O}_2/\text{Ar}$ flame. Filled squares – experimental data; curve 1 – modeling using reaction (a) [32]; curve 2 – modeling using reaction $\text{TTIP} + \text{H}_2\text{O} \rightarrow \text{Prod}$.

in [32]. The experimentally determined zone of $\text{Ti}(\text{OC}_3\text{H}_7)_4$ transformation is indeed much narrower.

It can be hypothesized that the primary stage of $\text{Ti}(\text{OC}_3\text{H}_7)_4$ conversion in the flame may proceed by two pathways through monomolecular decomposition reaction $\text{TTIP} \rightarrow \text{Prod}$, and the bimolecular hydrolysis reaction $\text{TTIP} + \text{H}_2\text{O} \rightarrow \text{Prod}$. To find out which of the two pathways is more probable, we calculated, by using the approach described in [43], the profile of TTIP consumption rate along the flame zone (Figs. S2–S4, Table S1, Supplementary data), based on the experimentally measured profiles of $\text{Ti}(\text{OC}_3\text{H}_7)_4$ concentration and of temperature (Figs. 1 and 2) and determined the rate constants of these two reactions.

In the case of monomolecular reaction, the Arrhenius parameters of the rate constant turned out to be $A = 3 \times 10^6 \text{ s}^{-1}$, $E_a = 13.6 \text{ kcal/mol}$, with an unreasonably low A value. At the same time, the Arrhenius parameters for the latter

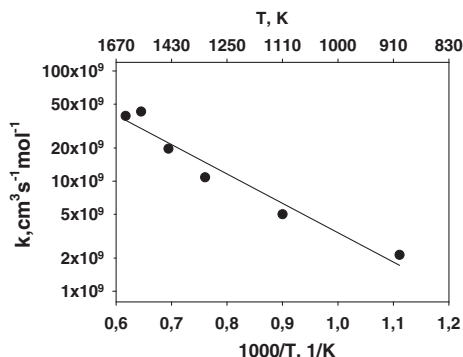


Fig. 3. Arrhenius plot for the experimental (filled circles) and extrapolated rate constant of the reaction $\text{TTIP} + \text{H}_2\text{O} \rightarrow \text{Prod}$.

bimolecular primary reaction were calculated to be $A = 2 \times 10^{12} \text{ mol}^{-1} \text{ cm}^3 \text{ s}^{-1}$, $E_a = 12.2 \text{ kcal/mol}$. Note that such value of A factor is typical of bimolecular reactions. The temperature dependence of this rate constant in Arrhenius coordinates is shown in Fig. 3. Figure 2 demonstrates that hydrolysis of $\text{Ti}(\text{OC}_3\text{H}_7)_4$ with the above mentioned rate constant perfectly describes the experimental concentration profile of TTIP in the flame (curve 2). Therefore, our results give the evidence that conversion of $\text{Ti}(\text{OC}_3\text{H}_7)_4$ in the flame occurs mainly via the hydrolysis reaction.

The results of quantum chemical calculations (B3LYP/6–311++G(2df,p)) support this conclusion. The stationary points on the potential energy surface (PES) corresponding to hydrolysis of TTIP and to the primary monomolecular reactions of its thermal decomposition are shown in Figs. 4 and 5, respectively. It is seen from Fig. 4 that the B3LYP calculations predict the effective activation barrier of the TTIP hydrolysis to be ca. 10 kcal/mol. This value is in a good agreement with the $E_a = 12.2 \text{ kcal/mol}$ estimated experimentally.

Three primary monomolecular decomposition reactions of TTIP were also considered. Two of them yield radicals, and the third reaction leads to molecular products (Fig. 5). Figure 5

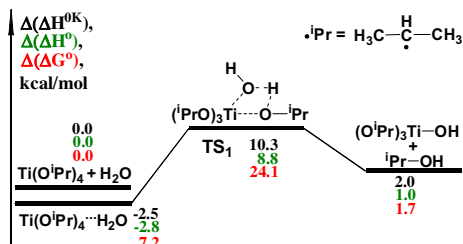


Fig. 4. The stationary points on the PES corresponding to hydrolysis of TTIP.

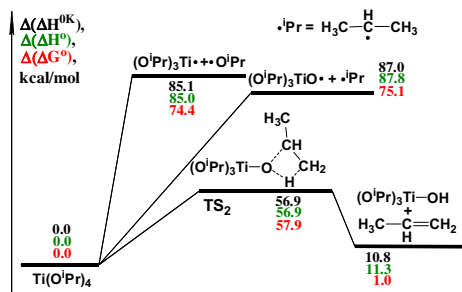


Fig. 5. The stationary points on the PES corresponding to monomolecular reactions of thermal decomposition of TTIP.

demonstrates that the barriers of reactions leading to the radical products (85–87 kcal/mol) are too high. The molecular decomposition yielding $\text{Ti}(\text{O}-\text{C}_3\text{H}_8)_3(\text{OH})$ and propene has a much lower activation barrier (56.9 kcal/mol, Fig. 5). This is the dominating primary unimolecular reaction of TTIP thermolysis, but its barrier is still too high to be responsible for very efficient decomposition of TTIP in the flame. Thus, it is clear that in the water-rich H_2/O_2 flame the reaction of hydrolysis (Fig. 4) dominates over the monomolecular decomposition.

The final product of TTIP decomposition in the flame is TiO_2 , which was detected by a molecular peak of 80 amu. Figure 6 shows the concentration profile of this mass peak normalized for the peak intensity of 20 amu (Ar^{2+}). The measurements were performed with the ionizing energy of 70 eV. As seen from this figure, formation of TiO_2 begins at a distance of 0.5 mm from the burner surface, with the maximum intensity of its peak reached at the distance of 2 mm.

Besides TiO_2 , seven other titanium-containing species were identified in the flame (Figs. 6–9): Ti (48 amu), TiH (49 amu), TiO (64 amu), TiOH (65 amu), HTiO_2 (81 amu), TiO_3 (96 amu), Ti_2O_3

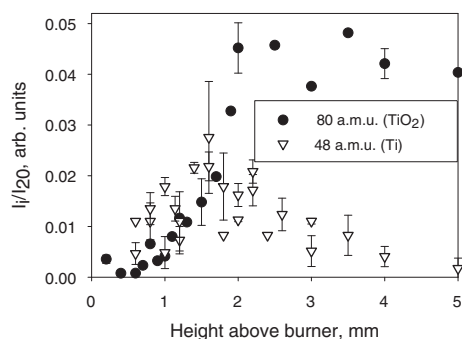


Fig. 6. Mass peak intensity profiles for the mass of 80 amu (TiO_2) and 48 amu (Ti) in $\text{H}_2/\text{O}_2/\text{Ar}$ flame with 0.12% $\text{Ti}(\text{OC}_3\text{H}_7)_4$ additive.

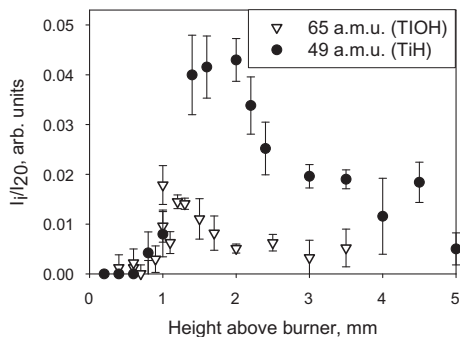


Fig. 7. Mass peak intensity profiles for the mass of 49 amu (TiH) and 65 amu (TiOH) in $\text{H}_2/\text{O}_2/\text{Ar}$ flame with 0.12% $\text{Ti}(\text{OC}_3\text{H}_7)_4$ additive.

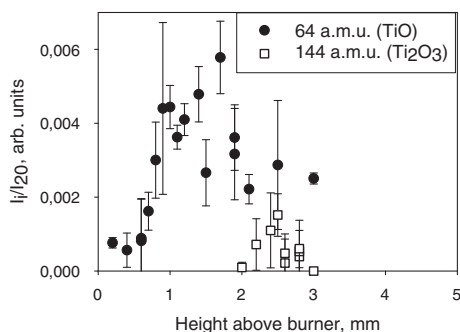


Fig. 8. Mass peak intensity profiles for the mass of 64 amu (TiO) and 144 amu (Ti_2O_3) in $\text{H}_2/\text{O}_2/\text{Ar}$ flame with 0.12% $\text{Ti}(\text{OC}_3\text{H}_7)_4$ additive.

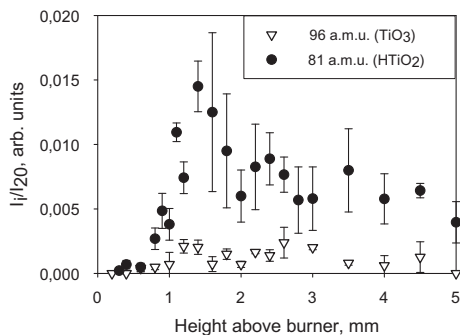


Fig. 9. Mass peak intensity profiles for the mass of 81 amu (HTiO_2) and 96 amu (TiO_3) in $\text{H}_2/\text{O}_2/\text{Ar}$ flame with 0.12% $\text{Ti}(\text{OC}_3\text{H}_7)_4$ additive.

(144 amu). The intensities of all these peaks, similarly to that of TiO_2 , were measured with the ionizing electron energy of 70 eV. As seen from the profiles obtained, the peak intensity maxima of those species are achieved at the following distances from the burner surface (Figs. 6–9 and

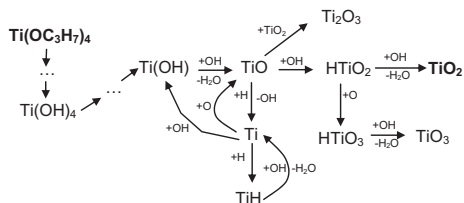


Fig. 10. The scheme of the main transformation reactions of $\text{Ti}(\text{OC}_3\text{H}_7)_4$ in $\text{H}_2/\text{O}_2/\text{Ar}$ flame.

Fig. S5, supplemental material): TiOH –1 mm, TiO –1.0–1.3 mm, HTiO_2 –1.3 mm, TiO_3 –1.4–1.5 mm, Ti –1.6 mm, TiH –1.8–2 mm, and Ti_2O_3 –2.5 mm. The TTIP is completely consumed at the distance of up to 1 mm from the burner surface (Fig. 2), and the maximum concentration of TiO_2 is reached at the distance of about 2 mm (Fig. 6). These facts confirm that the identified species are intermediates in the transformation chain $\text{Ti}(\text{OC}_3\text{H}_7)_4 \rightarrow \dots \rightarrow \text{TiO}_2$.

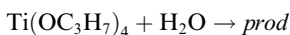
On the basis experimental data obtained, we infer that the sequential release of the isopropyl fragments from the $\text{Ti}(\text{OC}_3\text{H}_7)_4$ takes place in the flame reaction zone 0–1 mm from the burner surface. Most likely, the species with a structure of $\text{Ti}(\text{OH})_n$ are formed in this zone. Their subsequent reactions with active radical intermediates (OH , H , and O) yield Ti-containing species detected in this study (Figs. 6–9).

The proposed scheme of $\text{Ti}(\text{OC}_3\text{H}_7)_4$ transformations is presented in Fig. 10 and in Table S2, Supplemental data. This scheme is in agreement with the sequence of the concentration maxima of the corresponding Ti-containing intermediates.

The proposed mechanism does not claim to be complete. However, it describes well the conversion of the species observed in flame. Testing and further development of this scheme are complicated due to the absence of thermodynamic and kinetic data for the most part of titanium-containing species. Thermochemical data are available only for TiO , Ti , TiO_2 , and $\text{Ti}(\text{OH})_4$. Indeed, further work is necessary to test, complement, and correct this mechanism.

4. Conclusions

The chemistry of $\text{Ti}(\text{OC}_3\text{H}_7)_4$ combustion in $\text{H}_2/\text{O}_2/\text{Ar}$ flame was studied experimentally and computationally (numerical modeling and quantum chemical calculations). Based on the data obtained, a possible scheme of reactions was proposed, describing conversion of $\text{Ti}(\text{OC}_3\text{H}_7)_4$ and formation of TiO_2 in the flame studied. The reaction of hydrolysis



was proposed to be a primary stage of the TTIP conversion with a bimolecular rate constant

$$k = 2 \times 10^{12} \exp\left(-\frac{12.2 \text{ kcal/mol}}{RT}\right) \text{ mol}^{-1} \text{ cm}^3 \text{ s}^{-1}$$

Acknowledgements

This study was supported by the Russian Foundation of Basic Research (Grant No. 10-03-00442) and by the Siberian Supercomputer Center. V.G.K. also appreciates the support of this work by the Russian Ministry of Education and Science (project NK-187P6, contract # P1475), SB RAS (Lavrentiev grant programme), and the Government of the Novosibirsk region.

Appendix A. Supplementary data

Supplementary data associated with this article can be found, in the online version, at <http://dx.doi.org/10.1016/j.proci.2012.05.081>.

References

- [1] B. O'Regan, M. Gratzel, *Nature* 353 (1991) 737–740.
- [2] M. Gratzel, *Nature* 414 (2001) 338–344.
- [3] P.T. Moseley, *Sens. Actuators, B* 6 (1992) 149–156.
- [4] S. Akbar, P. Dutta, C.H. Le, *Int. J. Appl. Ceram. Technol.* 3 (2006) 302–311.
- [5] G.J. Wilson, G.D. Will, R.L. Frost, S.A. Montgomery, *J. Mater. Chem.* 12 (2002) 1787–1791.
- [6] T. Sugimoto, X.P. Zhou, *J. Colloid Interface Sci.* 252 (2002) 347–353.
- [7] J.M. Macak, H. Tsuchiya, A. Ghicov, P. Schmuki, *Electrochem. Commun.* 7 (2005) 1133–1137.
- [8] W. Li, S.I. Shah, C.P. Huang, O. Jung, C. Ni, *Mater. Sci. Eng. B* 96 (2002) 247–253.
- [9] E.D. Tolmachoff, A.D. Abid, D.J. Phares, C.S. Campbell, H. Wang, *Proc. Combust. Inst.* 32 (2009) 1839–1845.
- [10] M.S. Wooldridge, P.V. Torek, M.T. Donovan, et al., *Combust. Flame* 131 (2002) 98–109.
- [11] G.D. Ulrich, B.A. Milines, N.S. Subramanian, *Combust. Sci. Technol.* 14 (1976) 243–249.
- [12] H.F. Calcote, W. Felder, D.G. Keil, D.B. Olson, *Proc. Combust. Inst.* 23 (1990) 1739–1744.
- [13] M.R. Zachariah, S. Huzarewicz, *J. Mater. Res.* 6 (1991) 264–269.
- [14] M.R. Zachariah, M.I. Aquino, R.D. Shull, E.B. Steel, *Nanostruct. Mater.* 5 (1995) 383–392.
- [15] R.L. Axelbaum, C.R. Lottes, J.I. Huertas, L.J. Rosen, *Proc. Combust. Inst.* 26 (1996) 1891–1897.
- [16] C.B. Almquist, P. Biswas, *J. Catal.* 212 (2002) 145–156.
- [17] S.E. Pratsnis, W. Zhu, S. Vemury, *Powder Technol.* 86 (1996) 87–93.
- [18] S. Vemury, S.E. Pratsinis, *Appl. Phys. Lett.* 66 (1995) 3275–3277.

- [19] S. Vemury, S.E. Pratsinis, *J. Aerosol Sci.* 27 (1996) 951–966.
- [20] S. Vemury, L. Kibbey, S.E. Pratsinis, *J. Mater. Res.* 12 (1997) 1031–1042.
- [21] M.R. Zachariah, D.R.F. Burgess Jr., *J. Aerosol Sci.* 25 (1994) 487–497.
- [22] Y. Xing, U.O. Koylu, D.E. Rosner, *Combust. Flame* 107 (1996) 85–102.
- [23] S. Memarzadeh, E.D. Tolmachoff, D.J. Phares, H. Wang, *Proc. Combust. Inst.* 33 (2011) 1917–1924.
- [24] J. Wang, S. Li, W. Yan, S.D. Tse, Q. Yao, *Proc. Combust. Inst.* 33 (2011) 1925–1932.
- [25] R.H. West, M.S. Celnik, O.R. Inderwildi, M. Kraft, G.J.O. Beran, W.H. Green, *Ind. Eng. Chem. Res.* 46 (2007) 6147–6156.
- [26] R.H. West, R. Shirley, M. Kraft, C.F. Goldsmith, W.H. Green, *Combust. Flame* 156 (2009) 1764–1770.
- [27] R. Shirley, W. Phadungsukanan, M. Kraft, J. Downing, N.E. Day, P. Murray-Rust, *J. Phys. Chem. A* 114 (2010) 11825–11832.
- [28] T.-H. Wang, A.M. Navarrete-Lopez, S. Li, D.A. Dixon, J.L. Gole, *J. Phys. Chem. A* 114 (2010) 7561–7570.
- [29] R.H. West, G.J.O. Beran, W.H. Green, M. Kraft, *J. Phys. Chem. A* 111 (2007) 3560–3565.
- [30] B. Karlemo, P. Koukkari, J. Paloniemi, *Plasma Chem. Plasma Process* 16 (1996) 59–77.
- [31] S.E. Pratsinis, H. Bai, P. Biswas, M. Frenklach, S.V.R. Mastrangelo, *J. Am. Ceram. Soc.* 73 (1990) 2158–2162.
- [32] K. Okuyama, R. Ushio, Y. Kousaka, R.C. Flagan, J.H. Seinfeld, *AIChE J.* 36 (1990) 409–419.
- [33] T. Seto, M. Shimada, K. Okuyama, *Aerosol Sci. Tech.* 23 (1995) 183–200.
- [34] O.P. Korobeinichev, S.B. Il'in, V.V. Mokrushin, A.G. Shmakov, *Combust. Sci. Technol.* 117 (1996) 51–67.
- [35] W.E. Kaskan, *Proc. Combust. Inst.* 6 (1957) 134–141.
- [36] R.J. Kee, J.F. Grcar, M.D. Smooke, J.A. Miller, A Program for *Modeling Steady, Laminar, One-Dimensional Premixed Flames*, Sandia National Laboratories report SAND85-8240, 1985.
- [37] R.J. Kee, F.M. Rupley, J.A. Miller, *Chemkin II: A Fortran Chemical Kinetics Package for the Analysis of Gas-phase Chemical Kinetics*, Sandia National Laboratories report SAND89-8009, 1989.
- [38] A.A. Konnov, *Combust. Flame* 152 (2008) 507–528.
- [39] NIST Chemistry WebBook, NIST Standard Reference Database 69; Linstrom, P. J., Mallard, W. G., Eds.; National Institute of Standards and Technology, Gaithersburg, MD June 2005; <http://webbook.nist.gov/chemistry/>.
- [40] A.D. Becke, *J. Chem. Phys.* 98 (1993) 5648–5852.
- [41] C. Lee, W. Yang, R.G. Parr, *Phys. Rev. B* 37 (1988) 785–789.
- [42] Full citation of the Gaussian 03 code appears in the supplemental material, R1.
- [43] R.M. Fristrom, A.A. Westenberg, *Flame struct.*, McGraw-Hill, New York, 1964.